Available online at www.sciencedirect.com
SCIENCE DIRECT®
Journal of the European Ceramic Society 25 (2005) 2825–2828
www.elsevier.com/locate/jeurceramsoc

Ultraviolet excitation of photoconductivity in thin films of sol–gel SnO_2

V. Geraldo [a,b], L.V.A. Scalvi [a,*], E.A. Morais [a], C.V. Santilli [c], P.B. Miranda [b], T.J. Pereira [a]

[a] *Departamento de Física, FC-UNESP, C. Postal 473, 17033-360 Bauru, SP, Brazil*
[b] *Instituto de Física de São Carlos-USP, C. Postal 369, 13560-970 São Carlos, SP, Brazil*
[c] *Inst. Química de Araraquara, UNESP, C. Postal 355, 14801-907 Araraquara, SP, Brazil*

Available online 30 March 2005

Abstract

Tin dioxide (SnO_2) thin film photoconductivity spectra were measured for a large temperature range using a deuterium source. The intensity of photocurrent spectra in the range 200–400 nm is temperature dependent, and the photocurrent increases in the ultraviolet even for illumination with photon energies much higher than the bandgap transition. This behavior is related to recombination of photogenerated electron–hole pairs with oxygen adsorbed at grain boundaries, which is consistent with nanoscopic crystallite size of sol–gel deposited films.
© 2005 Elsevier Ltd. All rights reserved.

Keywords: Sol–gel processes; Electrical conductivity; Sensors; Tin dioxide

1. Introduction

Tin dioxide (SnO_2) is a wide bandgap semiconductor (forbidden gap in the range 3.5–4.0 eV[1]). When undoped, it presents n-type conduction due to the presence of oxygen vacancies and interstitial tin atoms. In the form of thin films, this material is characterized by high optical transmission.[2] The conjunction of optical and electrical properties make tin dioxide very attractive for many kind of applications in optoelectronic devices,[3] gas sensors[4,5] and solar collector.[6] SnO_2 film properties are strongly influenced by the preparation technique. The sol–gel route for obtaining SnO_2 thin films presents many advantages compared to other technique, such as excellent homogeneity, thickness control and possibility of coating large and complex surfaces, using both inorganic and organic precursors. However, the electrical properties of layers prepared by this process are worse compared to films deposited by other techniques. This worse performance is generally attributed to a combination of effects associated to nanosized grains of sol–gel materials. As shown in this paper, crystallites generated by our sol–gel dip-coating route have nanoscopic dimensions. Therefore, a considerable amount of crystallites is present in the material, which makes electron scattering at grain boundaries the most relevant mechanism to the film conductivity. Moreover, the presence of oxygen ionic species adsorbed at grain boundary may create a depletion layer as large as half of the grain width.[7] The physics of electronic conduction in these films is peculiar and rather unknown. Therefore, it deserves a careful investigation.

In this work, we present results concerning the electrical transport in nanocrystalline undoped SnO_2 thin films. Photocurrent spectra are obtained by using a deuterium source to irradiate the sample in the ultraviolet range, at low temperature. Spectra are normalized concerning the film optical absorption and the photon flux reaching the sample. The net result is the photoconductivity quantum yield, which shows marked temperature dependence.

2. Experimental

Colloidal suspensions of SnO_2 nanoparticles have been prepared from Sn^{4+} aqueous solution (0.25 mol l^{-1}) obtained by dissolving $SnCl_4 \cdot 5H_2O$ powder. Hydrolysis was promoted by adding ammonium hydroxide (NH_4OH) under magnetic stirring until pH reaches 11. The obtained precipitated was submitted to dialysis against distilled water in order to elimi-

* Corresponding author. Tel.: +55 14 3103 6084; fax: +55 14 3103 6094.
E-mail address: scalvi@fc.unesp.br (L.V.A. Scalvi).

0955-2219/$ – see front matter © 2005 Elsevier Ltd. All rights reserved.
doi:10.1016/j.jeurceramsoc.2005.03.149

nate as much as possible chloride and ammonium ions. These suspensions were used for film deposition on silicate glass substrates by dip-coating technique, with a withdrawing rate of 10 cm/min. After each dip, the deposited film was fired at 400 °C for 10 min. When the number of 30 layers was reached, films were annealed at 550 °C for 1 h under air, resulting in a thickness of about 250 nm.

To perform electrical measurements, indium electrodes have been evaporated on the samples through a shadow mask in an Edwards evaporator system. Electrodes were annealed to 150 °C for 20 min in air. Low temperature electrical measurements were done in an Air Product Cryostat that controls temperature in the range 25–300 K to within 0.1 K.

For photoconductivity (pc) spectrum measurements, illumination was provided by a 30 W deuterium lamp coupled to a computer controlled ultraviolet monochromator. The photocurrent was continuously recorded with a 6517 A Keithley electrometer. The measured photocurrent was normalized by the photon flux in order to eliminate the dependence of the pc excitation upon the incident light intensity and sample absorption coefficient. This procedure allows the calculation of the photoconductivity quantum yield (PCQY):

$$\mathrm{PCQY} = I_{\mathrm{pc}}(\mathrm{Abs} \times N_{\mathrm{ph}})^{-1} \quad (1)$$

where I_{pc} is the photocurrent (A), Abs is the film absorbance spectrum and N_{ph} is the number of photons reaching the sample as function of wavelength of irradiating monochromatic light. N_{ph} was obtained by taken into account the light that effectively reaches the film, measured by a photodetector placed at same position of the film in the optical set-up, divided by the detector response and the energy of illuminating monochromatic light. PCQY may be interpreted as the measured photocurrent normalized by the number of photons effectively absorbed by the film.

X-ray diffraction measurements were carried out with a Rigaku diffractometer coupled with Cu Kα radiation (λ = 1.5418 Å) operating under 40 kV and 20 mA, at detection rate of 3° min^{-1} with a 0.02° step.

3. Results and discussion

Fig. 1 shows the X-ray powder diffraction patterns of the SnO_2 film. Besides the diffuse shape of peaks profile, typical of small crystalline domains, the cassiterite type structure[8] can be recognized by its three most intense peaks, which are labeled in Fig. 1. The average domains size, determined from line broadening in the pattern was about 5 nm. The quite small size of these crystallites leads us to believe that grain boundary defects have an important contribution to film conductivity.[9] It is well-known that the ultrafine crystals in the metal oxide semiconductor films lead to unusual properties arising from the quantum confinement effects and high surface area, which is essential for gas sensor application. In the following, we show that the fine-scaled microstructure of these films leads to unusual photoconduction behavior.

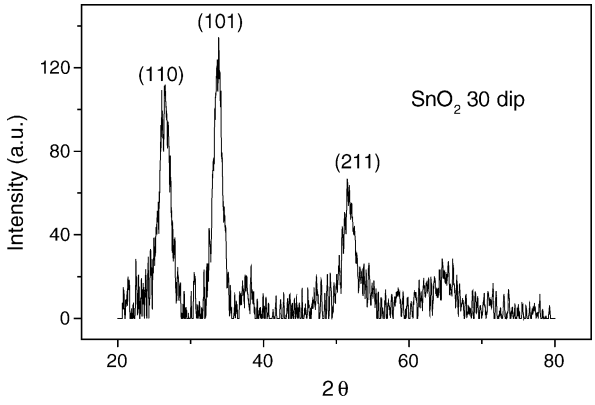

Fig. 1. X-ray diffraction data for undoped SnO_2 deposited by dip-coating sol–gel.

Fig. 2 shows the room temperature photoconductivity quantum yield in the range 200–400 nm for an undoped SnO_2 thin film. The PCQY increases from 350 nm and keeps increasing until about 220 nm. The measured photocurrent at room temperature is of order of μA. The variations in incident light intensity have no influence on the pc quantum yield, as it can be easily seen by comparing its shape with the incident intensity spectrum (inset of Fig. 2). The shoulder about 265 nm in the quantum yield cannot be associated to a peak in the lamp spectrum, since the influence would be

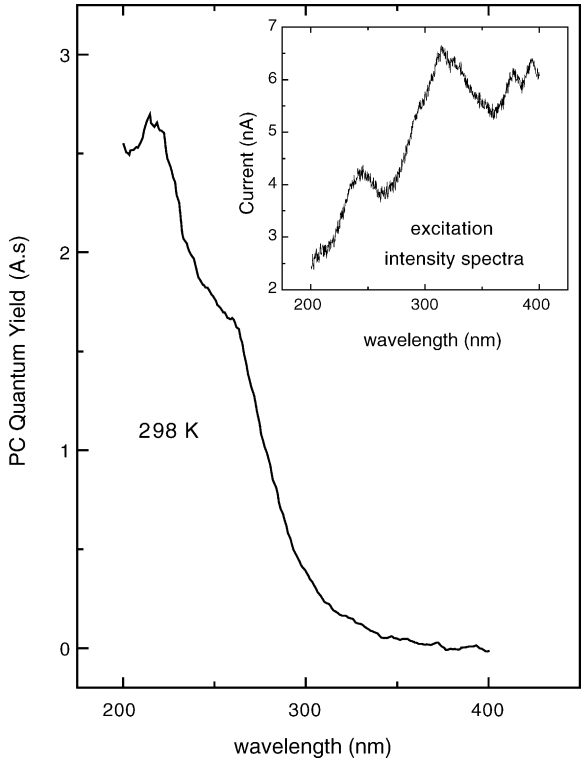

Fig. 2. Photoconductivity excitation spectra for and undoped SnO_2 thin film at room temperature. Inset: excitation intensity spectra.

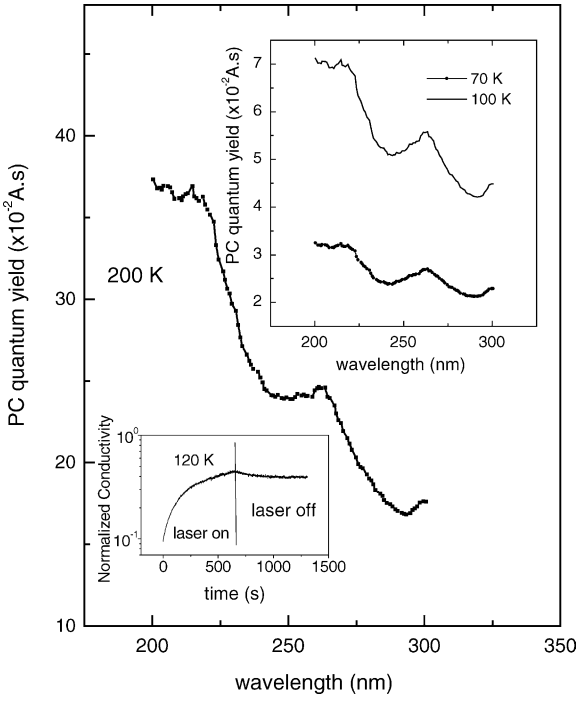

Fig. 3. Photoconductivity excitation spectra for and undoped SnO_2 thin film at 200 K. Superior inset: photoconductivity excitation spectra at 70 and 100 K. Lower inset: normalized conductivity as function of time of an undoped SnO_2 thin film, for excitation with the fourth harmonic of a Nd:YAG laser (266 nm), at 120 K.

much more pronounced in the range 300–400 nm, which was not observed.

Fig. 3 shows the PCQY for several temperatures. The main Fig. 3 shows the result for 200 K and the superior inset in Fig. 2 displays photocurrent measurement for 100 and 70 K. They are shown separately for better comparison due to quite different magnitude, since the lower the temperature, the lower the photocurrent signal. These results indicate that the electron capture increases with temperature decreases, which is typical of semiconductor behavior. The shoulder located at 265 nm, observed at room temperature, becomes a peak when the temperature is decreased. The low power of the deuterium source (30 W prior to monochromator, on the order of μW at the sample) does not allow the conductivity to increase very much. The dynamic equilibrium of optical ionization and thermal capture is dominated by the electron trapping in this case. Fig. 3 shows only the spectra in the range 200–300 nm because the low magnitude of measured current at these lower temperatures, combined with the low absorption coefficient of the samples in the range 300–400 nm, lead to artifacts on the PCQY due to normalization procedure for wavelengths longer than 300 nm. The lower inset in Fig. 3 shows the effect of illuminating the undoped SnO_2 film with the fourth harmonic of a Nd:YAG pulsed laser (266 nm), at 120 K. The pulsed laser is irradiated onto the sample though quartz windows. The pulse duration at 266 nm is about 6 ns and the pulse energy is 4.8 mJ. The pulse repetition rate is 10 Hz. Although we have previously published a temperature dependence study of laser excitation on sol–gel SnO_2 films,[10] this result was reproduced here for sake of clarity because this important ultraviolet excitation result helps the understanding of photoconductivity spectra reported in this paper. The conductivity increases up to one order of magnitude under laser excitation, until saturation, and remains constant after the illumination is removed.

With the normalization provided on the photocurrent by the PCQY calculation, the dependences of the pc excitation spectrum of Figs. 2 and 3 upon both the spectrum of the incident light reaching the sample and the undoped SnO_2 optical absorption spectra are eliminated. Therefore, changes in the pc quantum yield may be interpreted as due to variation of photogenerated carrier density, mobility and/or lifetime. The gradual increase in the PCQY for excitation wavelengths below 300 nm may be associated with changing carrier concentration and mobility in these films. The enhanced conductivity results from variation of free electron density plus decrease of space charge layer at grain boundaries. Both effects are related to photoinduced release of adsorbed oxygen, which is removed from the chamber by vacuum pumping. The system is kept under 10^{-5} Torr of pressure and the amount of gaseous oxygen available to react with free electrons is reduced. This participation of oxygen in the recombination becomes evident when we consider that even far from the bandgap transition (3.5–4.0 eV), the light energy keeps promoting an increase of conductivity. If the increase of conductivity were only due to electron–hole pair excitation, the recombination of these charge carriers for illumination with energies rather above the bandgap transition should decrease the conductivity, due to absence of available electronic states. Moreover, the excitation system has intensity practically negligible at short wavelength range, which is seen in the inset of Fig. 2. The combination of these two effects should lead to a decrease in the photoconductivity. The actual observed behavior must include electron and hole trapping by oxygen species since desorption and adsorption are slower process than electron–hole recombination because they depend on atomic diffusion into the sample (which is helped by the porosity of this material: 33%) and displacement of gaseous oxygen along the surface. The lower inset in Fig. 3 shows the slow increase of conductivity upon illumination of the SnO_2 film. We note that keeping the temperature constant and removing the illumination leads to a practically constant conductivity value, called persistent photoconductivity (PPC).[10–12] Conductivity varies again only when temperature is increased, but the room temperature value is recovered only a few hours later. The explanation of this PPC effect is related to the recombination of adsorbed oxygen with photogenerated electrons and holes[10]. Although the higher conductivity is a metastable effect caused by intense laser illumination, when light is removed the conductivity does not return to its original value because the oxygen released from the film is continuously eliminated by vacuum pumping. This is also observed in the photoconductivity spectra, since the

high conductivity value does not decrease even for illumination energies much higher than the bandgap transition.

The peak observed in the PCQY at low temperature, shown in Figs. 2 and 3, located about 265 nm is a striking result since it coincides with the excitation wavelength that induces PPC in undoped SnO_2 sol–gel films. The effect of decreasing PCQY intensity with temperature means that carriers are much more efficiently grounded to donor levels and the low light intensity is not enough to excite high photoconductivity effect. The much more intense laser light excitation confirms it, since it induces high conductivity for lower temperature, as we have previously shown.[10]

4. Conclusion

Variation of photoconductivity with excitation wavelength was measured using a deuterium source. These spectra are measured for the first time as function of temperature. Normalization by the photon flux reaching the sample leads to increasing photocurrent for illumination with monochromatic light of increasing energy. The photocurrent quantum yield has an onset at the absorption edge and continues to increase even for photon energies much higher than the bandgap transition. This phenomenon was related to recombination of photogenerated electron–hole pairs with adsorbed oxygen.

The nanosized grains of sol–gel dip-coated SnO_2 films increase participation of the oxygen adsorbed species in the electron and hole recombination processes explaining the observed photoinduced behavior and the high resistivity of these materials.

Acknowledgments

The authors wish to thank Prof. Ligia O. Ruggiero and Margarida J. Saeki for the help with the technical set-up, and CAPES, FAPESP, CNPq and MCT – PRONEX for the financial resources.

References

1. Ray, S. C., Karanjai, M. K. and Dasgupta, D., Tin dioxide based transparent semiconducting films deposited by the dip-coating technique. *Surf. Coat. Technol.*, 1998, **102**, 73–80.
2. Dien, E., Laurent, J. M. and Smith, A., Comparison if optical and electrical characteristics of SnO_2-based thin films deposited by pyrosol from tin precursors. *J. Eur. Ceram. Soc.*, 1999, **19**, 787–789.
3. Terrier, C., Chatelon, J. P. and Roger, J. A., Electrical and optical properties of Sb:SnO2 thin films obtained by the sol–gel method. *Thin Solid Films*, 1997, **295**, 95–100.
4. Guglielmi, M., Menegazzo, E., Paolizzi, M., Gasparro, G., Ganz, D., Putz, J. *et al.*, Sol–gel deposited Sb-doped tin oxide films. *J. Sol–Gel Sci. Technol.*, 1998, **13**, 679–683.
5. Nakata, S. and Ojima, N., Detection of a sample gas in the presence of an interferant gas based on a nonlinear response. *Sens. Actuators*, 1999, **B56**, 79–84.
6. Sanon, G., Rup, R. and Mansingh, A., Band-gap narrowing and band structure in degenerate tin oxide (SnO_2) films. *Phyical. Rev. B*, 1991, **44**, 5672–5680.
7. Watson, J., Ihokura, K. and Coles, G. S. V., The tin dioxide gas sensor. *Meas. Sci. Technol.*, 1993, **4**, 711–719.
8. *Powder Diffraction File, Inorganic, Vol 21*, JCPDS, Swathmore, 1983.
9. Messias, F. R., Vega, B. A. V., Scalvi, L. V. A., Siu Li, M., Santilli, C. V. and Pulcinelli, S. H., Electron scattering and effects of sources of light on photoconductivity of SnO_2 coatings prepared by sol–gel. *J. Non-cryst. Solids*, 1999, **247**, 171–175.
10. Morais, E. A., Scalvi, L. V. A., Geraldo, V., Scalvi, R. M. F., Ribeiro, S. J. L., Santilli, C. V. *et al.*, Electro-optical properties of Er-doped SnO_2 thin films. *J. Eur. Ceram. Soc.*, 2004, **24**, 1857–1860.
11. Mooney, P. M., Deep donor levels (DX centers) in III–V semiconductors. *J. Appl. Phys.*, 1990, **67**, R1–R26.
12. Ghosh, S. and Kumar, V., Confirmation of metastable neutral DX^0 state of Si-related DX center in $Al_xGa_{1-x}As$ by transient photoconductivity. *Solid State Commun.*, 1997, **104**, 781–785.